N87-26425

ULTRALIGHT AMORPHOUS SILICON ALLOY PHOTOVOLTAIC MODULES FOR SPACE APPLICATIONS

J.J. Hanak, Englade Chen, C. Fulton, and A. Myatt
Energy Conversion Devices, Inc.
Troy, Michigan

and

J.R. Woodyard
Wayne State University
Detroit, Michigan

Ultralight modules based on amorphous silicon alloys have been described recently as potentially useful for photovoltaic (PV) space arrays (ref. 1). They consist of thin-film multijunction solar cells deposited on polymeric substrates and interconnected in series and in parallel in a monolithic manner. Because of their extreme thinness, as small as 8 μm, very high specific power, in excess of 2.4 kW/kg and high stowability of 6.5 MW/m^3 have already been achieved. The modules are also flexible, so that they can be rolled up repeatedly to diameters of 3 cm or less. They are highly tolerant of physical damage, such as piercing by projectiles. They show improved radiation resistance to 1-MeV electrons and protons, by as much as 3 and 50 times, respectively, compared with crystalline Si and GaAs cells and also an improvement over $CuInSe_2$. Decreases in performance from exposure to light and ionizing radiation can be completely reversed by annealing at 160 to 200°C. Therefore, use of deployable and retractable arrays is proposed, which would not use glass covers and instead could be periodically annealed by solar heat inside their canisters. The monolithic structure facilitates design and fabrication of high voltage arrays required for high power systems. Large gains have also been made in the conversion efficiency and stability of a-Si alloy cells. A 13% AM1 efficiency and excellent optical stability have been already reported in devices consisting of a triple stacked cell structure and dual band gap materials a-Si:F:H and a-Si:Ge:F:H. AMO efficiency of 10% has been measured over active areas for similar cells. An update is given on the progress in this rapidly developing field, with emphasis on irradiation damage with 0.2 and 1-MeV protons and subsequent annealing behavior. Conceptual designs of large arrays, up to 1 MW, based on present engineering data are also presented.

INTRODUCTION

The development of ultralight, large-area, monolithic, flexible, roll-up modules, reported recently (ref. 1), is based on the unusual properties of the a-Si alloys and the rapid advances in PV technology based on them. Because of their very high optical absorption, solar cells made of a-Si alloys are less than one micrometer thick and their specific power exceeds 60 kW/kg, which is by far greater than for any crystalline material. Recent advances in device performance include exceeding of AM1 conversion efficiency of over 11% for single, wide-bandgap NIP cells of a-Si:F:H and reaching 10% with narrow-gap

*This work has been done for Sovonics Solar Systems

a-Si:Ge:F:H NIP cells (2, 3). These cells play an important role in achieving high efficiency with spectrum-splitting, multijunction devices. Next is the development of multijunction (ref. 4), multigap cells which have yielded AM1 efficiency of 13% with excellent stability (ref. 5). Efficiency of 30% has been forecast for such cells (ref. 6). The third is the achievement of excellent optical stability (ref. 7) with Sovonics multijunction cells using fluorine in the alloys (ref. 8). The fourth is the development of monolithic solar cell panel (ref. 9). The fifth is the development by Sovonics Solar Systems of a roll-to-roll continuous deposition process for multijunction cells onto a moving web (ref. 10). The sixth finding is that a-Si cells are about 3 times as resistant to 1-MeV electrons and more than 50 times to 1-MeV protons than crystalline silicon and GaAs and that the damage can be easily annealed out (refs. 11, 12, 13).

REVIEW OF THE FABRICATION AND THE FEATURES OF THE ULTRALIGHT MODULE

A summary of the description of the fabrication and of the features of the ultralight module published recently (ref. 1) follows. In order to take advantage of the high specific power inherent in the a-Si alloy solar cells, PV cell structures have been formed on thin foil substrates having thicknesses from 7.5 to μ25 m. The substrates included thin metals, metals clad with polyimide and polyimide films. A convenient thin metal substrate is electroformed nickel (ref. 14) or stainless steel, thinned by etching. The preferred substrate used in the present work for stowable, ultralight arrays is polyimide. Previous use of polyimide substrates has been limited to single cells and only of modest size (ref. 15). Normally, textured metal layers were coated on the substrates to enhance reflectively and promote light trapping (ref. 16). The material for the fabrication of the modules was produced by the Sovonics process (ref. 10) for continuous roll-to-roll deposition of thin-film, tandem-junction, PV cells onto webs 35 cm wide over 300 m long. A continuous layer of indium-tin oxide (ITO), about 60 nm thick, serving as the top transparent electrode was deposited by another roll-to-roll process.

A monolithic PV module structure has been designed which employs series and parallel cell interconnections (refs. 1, 17, 18) shown in figure 1. In this design the effect of an electrical shorting defect on the performance of the module is essentially limited to the defective cell. An analysis of such defects in the series-parallel module design is given elsewhere (ref. 19).

The processes for the fabrication of the module consisted of patterning of the continuous, deposited layers into arrays of cells by masking and etching or by scribing, screen-printing of current-collecting grids of silver paste, which also act as cell interconnections, application of electrical terminals, and encapsulation in polymeric sheets by lamination, as described in greater detail elsewhere (ref. 14).

To date, only single-gap a-Si:F:H alloys and single- or tandem- junction PV cell structures have been used for the development of the ultralight modules. Monolithic modules up to 61 x 30.5 cm^2 in area have been made on substrates 7.5 um thick, with or without top encapsulation, including a 37.5 m thick polyester or Tedlar. The module consists of 20 parallel strings of cells, with 12 cells in series per string, each cell having an area of 6 cm^2. PV performance data for the best module are given in table I. A comparison with specific power data reported by NASA for developmental "blankets" (ref. 22) and

NASA milestones for 1995 (ref. 23) with stowability data are shown in figures 2 and 3, respectively.

A photograph of an ultralight module in a roll, clearly demonstrating the features of flexibility, high specific weight, portability and stowability is shown in fig. 4. Another feature is the tolerance to physical damage, such as piercing by projectiles (ref. 1).

Because of the small thickness, such modules can be rolled up and unrolled repeatedly, without damage, to diameters as small as 3 cm (ref. 26). The results of such a test in which a module 31 cm x 31 cm in area and 50 μm in total thickness are shown in fig. 5.

CHARACTERISTICS AND PV PERFORMANCE OF PV CELLS AND MODULES

Although excellent progress has been made toward achieving high performance for the ultralight, monolithic modules, higher power output per area is needed to compete with existing PV arrays used in space. An intensive program has been underway at Sovonics toward developing advanced a-Si alloy materials and PV multijunction cell structures having high efficiency and stability. The status of this effort has been reported previously (refs. 2, 3, 5, 7, 20, 21) and the highlights are given in table II.

As indicated, the data in tables I and II are for AM1 illumination. Samples of 1-cm^2, dual-gap, triple cell, having AM1 active area efficiency of 12.5% have been measured at JPL by B. Anspaugh at AMO and shown to have a 10.0% efficiency (9.1% for total area) as shown in fig. 6.

SURVIVABILITY OF a-Si ALLOY SOLAR CELLS

A prerequisite for space PV arrays is a continuous operation over extended periods of time, ranging from days to tens of years, in the harsh environment of photon, electron and proton irradiation, bombardment by atomic oxygen, extremes of temperature excursions and physical damage due to surrounding equipment or meteorites. For high power arrays, high voltage arrays must be developed. Some of these issues have been addressed here and elsewhere, with remarkable success as described below.

Optical Stability of Multijunction PV Cells

Outstanding progress has been reported in achieving optical stability in Sovonics multijunction, dual-gap PV cells (refs. 5, 21) with respect to the Staebler-Wronski effect. Results for a triple-stacked, dual-gap cell with initial efficiency of 11.2% retained over 90% of its initial performance after 2500 hours of continuous illumination.

Stability of a-Si Alloy Cells in Ionizing Radiation

Studies of the effect of 1-MeV electrons on a-Si:H cells up to a fluence of 10^{16} electrons cm^{-3} have indicated approximately a threefold tolerance, compared with crystalline silicon cells (refs. 11, 12). Moreover, the damage was found to be fully annealable under conditions used to anneal the S-W effect.

Irradiation studies with 1-MeV protons (ref. 13) have been reported with fluences ranging from 10^{11} to 1.6×10^{15} cm^{-2} on single cells of a-Si:F:H, a-Si:Ge:F:H, and single-gap, tandem-junction cells of a-Si:F:H*. More than a 50-fold greater tolerance to this radiation has been found in comparison with crystalline silicon and GaAs (ref. 24). Moreover, a total recovery of conversion efficiency has been attained after a one-hour anneal at 160°C, for fluences up to 10^{14} and 75% recovery for fluences up to 10^{15}. After 3-hour and 23 hour anneals, 90% and 97% recoveries, respectively, are reported for fluence of 10^{15} protons cm^{-2}. These results are shown again for the single-gap, a-Si:F:H tandem cells in fig. 7.

Additional radiation experiments with 200-keV protons have been reported (ref. 26) on the same set of samples after the annealing treatment. The effect of 200-keV proton irradiation on the performance of the three types of cell studied is shown in fig. 8, which also includes data for 1-MeV protons from reference 13. A comparison of the 1-MeV and 200-keV irradiation data for the dual-gap tandem cells alone is shown in fig. 9. A comparison with fig. 8 shows that the results are very similar to the single-gap a-Si:F:H tandem cells. As expected from other work (ref. 25), the lower-energy protons give rise to a somewhat increased rate of damage than for 1-MeV protons. The relative radiation tolerance to 200-keV protons is still much greater than for crystalline silicon or GaAs solar cells (refs. 24, 25). Figure 10 gives a comparison for irradiation of crystalline Si, GaAs, $CuInSe_2$ and a-Si alloy cells with 1-MeV protons and shows superior radiation resistance of the a-Si alloy, dual-gap, tandem cells.

The results of the annealing experiments on the tandem cells for the 200-keV proton irradiation are shown in fig. 11. Results are shown for various temperatures and times as a function of fluence. As with the 1-MeV proton irradiation shown in fig. 7, the damage is fully annealable at a modest temperature of 160°C up to a fluence of 10^{14} cm^{-2} and up to 79% of initial efficiency at 10^{15} cm^{-2}.

We have considered some of the mechanisms which lead to the decrease of the efficiency resulting from proton bombardment. Figures 8 and 9 show that 200-keV protons of a given fluence have about the same effect on the relative efficiency as 1-MeV protons with ten times the fluence. Thus the relative efficiency curves of the 1-MeV proton irradiations, when shifted to the left by one order of magnitude in fluence, compare favorably with the 200-keV data except for the highest fluences. Table III shows the results of our calculations to determine the nuclear recoil cross sections for the displacement of the various atoms in the cells. Displacement energies of 3.5 eV for hydrogen and 13 eV for Si and Ge were used in the calculations and only primary collisions are considered. The displacement cross sections are about five times larger at 200-keV as compared with 1-MeV. There are deficiencies in the analysis due to the uncertainty in the displacement energies, the electronic stopping of the protons and the displacement of atoms by the recoiling atoms. We believe that the agreement is adequate to suggest that the reduction in the relative efficiency is due to defects created by nuclear collisions. Our measurements show that the V_{oc} is insensitive to the proton fluence suggesting that the defects are produced primarily in the intrinsic region of the cell. Further confirmation of the suggestion is manifested by the relative effect of the protons on cells with different thicknesses; the

*In Reference 13, the proton radiation results for the tandem-junction cells have been reported by error as for tandem-junction, dual-gap cells.

measurements show that protons of the same energy and fluence degrade the efficiency of thicker cells to a greater extent.

The cells have been isochronally annealed for three hours at temperatures in the range of 60 to 160°C in an effort to determine if the knock-on of hydrogen or Si and Ge results in the defects. In a simple model where the protons are assumed to knock-on the hydrogen and create dangling bonds, the bonds should be passivated by the diffusion of hydrogen upon annealing. If this were the case, the annealing data should behave in a simple Arrhenius fashion. Our annealing data cannot be characterized by an Arrhenius plot over the range of fluences we studied; an approximate fit to an Arrhenius plot can be obtained at low fluences with an activation energy of the order of 0.1 eV. At higher fluences the cells are very resistant to isochronal annealing except at 160°C. We therefore conclude that the primary mechanism for the reduction of the relative efficiencies is not the creation of dangling bonds by the displacement of hydrogen. The complexity of the annealing data suggests that the defects are created by the displacement of Si and Ge and that a number of different types of defect configurations are produced by the recoiling atoms. The resistance to annealing at the higher fluences may be due to the overlapping of the damage zones; ion implantation studies show that damage produced at fluences where the damage zones overlap is more resistant to annealing than damage produced at fluences sufficiently low to insure that the damage zones do not overlap. If our suggestion is correct we expect that tandem cells made from several thin PIN tandems should be more radiation resistant than either tandems or single PINs made with thick intrinsic layers. An analysis of Figures 7, 8 and 9 confirms this suggestion.

High Voltage Arrays

In the monolithic structure of the ultralight modules shown in fig. 1 the cells as well as the cell interconnections are encapsulated in a continuous, transparent flexible cover, so that no bare electrical leads are exposed to the external environment. This structure is very amenable to design and fabrication of a high-voltage array.

CONCEPTUAL DESIGN OF LARGE SPACE ARRAYS

Because of high radiation resistance of Sovonics solar panels with respect to 1-MeV electron and 1-MeV and 200-keV proton irradiation and high optical stability, it appears that protection of the a-Si alloy PV arrays by cover glass is not required. Instead, the use of rollup, deployable and retractable arrays is recommended, so that if necessary, the arrays can be annealed periodically in their canisters under modest conditions of time and temperature. An example of such a concept is shown in fig. 12. A system of this type would be useful for electrical propulsion of vehicles which would be used to traverse high radiation zones, such as future Earth-Moon shuttles.

Another concept design, shown in figure sequence 13 a, b, c, and d, is for a 1 megawatt array, either for defense purposes or for interplanetary electrical propulsion.

CONCLUSIONS

Ultralight and ultrathin, flexible, rollup monolithic PV modules have been developed consisting of multijunction, amorphous silicon alloys for either terrestrial or aerospace applications. The rate of progress at Sovonics of increasing conversion efficiency of stable multijunction and multigap PV cells indicates that arrays of these ultralight modules can be available for NASA's high power systems for the 1990's. Already NASA's goals for specific power for 1990's have been nearly doubled. Because of the extremely light module weight and highly automated process of manufacture, the monolithic a-Si alloy arrays are expected to be strongly competitive with other systems, either photovoltaic, solar dynamic or nuclear for use in NASA's Space Station or other large aerospace uses in the years to come. For similar reasons extensive use of the monolithic ultralight arrays is expected for terrestrial applications as mobile high-power supplies.

REFERENCES

1. J. J. Hanak, Conf. Record 18th IEEE PVSC, 1985, 89.
2. S. R. Ovshinsky and J. Young, SPIE Proceedings, Vol. 706 edited by David Adler (SPIE, Bellingham, WA, 1986) in press.
3. J. Yang, T. Glatfelter, J. Burdick, J.P. Fournier, L. Boman, R. Ross and R. Mohr; Proceedings of the 2nd International PVSEC, Beijing, China, 1986, p. 361.
4. J. J. Hanak, J. Non-Cryst. Solids, 35 & 36, 755 (1980), North-Holland Publishing Co.,; Y. Hamakawa, H. Okamoto and Y. Nitta, ibid., 749.
5. Jeffrey Yang, Robery Ross, Ralph Mohr, and Jeffrey Fournier, 1986 Materials Research Society Spring Meeting, Palo Alto, CA.
6. Stanford R. Ovshinsky, Tech. Digest Int. PVSEC-1, Kobe, Japan, Nov. 13-16, 1984, 577.
7. J. Yang, R. Mohr and R. Ross, Tech. Digest Int. PVSEC-1, Kobe, Japan, Nov. 13-16, 1984, Late News, A-II-L 6.
8. S. R. Ovshinsky and A. Madan, Nature 276, 482 (1978).
9. J. J. Hanak, Solar Energy, 23, 1456 (1979).
10. Masat Izu and S. R. Ovshinsky, Thin Solid Films, 119 (1984); S. R. Ovshinsky, Proc. SPIE 407, 5 (1983); Masat Izu and S. R. Ovshinsky, ibid., 42.
11. C. F. Gay, R. R. Potter, D. P. Tanner and B. E. Anspauch, Conf. Record 17th IEEE PVSC, 1984, 151.
12. C. E. Byvik, W. Slemp, B. T. Smith and A. M. Buonchristiani, ibid., 155.
13. J. J. Hanak, A. Myatt, Prem Nath, and J. R. Woodyard, Conf. Record 18th IEEE PVSC, 1985, 1718.
14. H. Okaniwa, M. Asano, K. Nakatano, M.Yano, and K. Suzuki, Jpn. J. Appl. Phys. Suppl. 21-22 (1982) 239.
15. J. J. Hanak, M. Izu, Prem Nath and J. Young, U.S. Patent 4,530,739, July 23, 1985.
16. H. W. Deckman, C. B. Roxlo, C. R. Wronski, and E. Yablonovitch, Conf. Record 17th IEEE PVSC, 1984, 955.
17. Yuan-sheng Tyan and Evelio A. Perez-Albuerne, ibid., 961.
18. J. J. Hanak, U.S. Patent 4,514,579, April 30, 1985.
19. Troy Glatfelter and W. Czubatyj, Conf. Record 18th IEEE PVSC, 1985, 1186.
20. Prem Nath and M. Izu, ibid., 939
21. S. Guha, J. Non-Cryst. Solids 77-78, 1451 (1985).
22. D. J. Flood, private communication.

23. J. P. Mullin, J. C. Loria and H. W. Brandhorst, Conf. Record 17th IEEE PVSC, 1984, 12.
24. B. E. Anspaugh and R. G. Downing, ibid., 23.
25. J. Y. Yaung, Space Photovoltaic Research and Technology 1983, NASA Conference Publication 2314, p.56.
26. J. J. Hanak, C. Fulton, A. Myatt, Prem Nath, and J. R. Woodyard, 21st IECEC, San Diego, CA, August 25-29, 1986.

Table I
PV Data of a-Si Alloy Ultralight Module at AM1
(Area = 61 x 30.5 cm^2)

Voc	16.4 V
Isc	1.05 A
Fill Factor	0.56
Power	9.69 W
Power/weight	2.4 kW/kg
Power/area	52 W/m^2
Power/Volume	6.5 MWm^3

Table II
Highlights of the Status of Sovonics PV Cells

AM1 Conversion Efficiency (%)	Cell Type	Size (cm^2)	Reference
13.0	dual-gap, triple	1	5
12.0	single-gap, triple	1	2
11.1	dual-gap, triple	930	20
12.5	dual-gap, tandem	1	5
10.4	dual-gap, tandem	930	20
11.8	single-gap, tandem	1	2
9.0	single-gap, tandem	*	21

*35-cm wide, continuous web, in production

Table III
Results of Cross Section Calculations

System	Energy	E_d	$\sigma(\Delta Q)$
H→ H	200 keV	3.5 eV	9.3E-20 cm^2
H→ Si	200 keV	13 eV	1.8E-19 cm^2
H→ Ge	200 keV	13 eV	3.5E-19 cm^2
H→ H	1.00 MeV	3.5 eV	1.9E-20 cm^2
H→ Si	1.00 MeV	13 eV	3.4E-20 cm^2
H→ Ge	1.00 Mev	13 eV	6.9E-20 cm^2

Figure 1. Monolithic module structure consisting of four parallel strings of four series-connected cells in each string.

Figure 2. Specific power data for various types of PV modules or "blankets".

Figure 3. Stowability data for PV modules and blankets.

Figure 4. Ultralight, monolithic PV module on a roll (module only on the top three wraps); a full roll would have a power output of about 35 kW, compared with 10 kW for the diesel generator in the background.

Figure 5. Test of the effect of repetitive rolling and unrolling of an ultralight module around a cylindrical mandril on its PV performance.

Figure 6. Current-voltage and cell performance data for dual-gap, triple stacked cell under AMO illumination (for active cell area).

Figure 7. The effect of 1-MeV proton irradiation on the conversion efficiency of tandem, single-gap, a-Si:F:H cells and the effect of subsequent annealing at $160^{o}C$ (ref. 13).

Figure 8. The effect of 200-keV and 1-MeV proton irradiation on the conversion efficiency of single a-Si:F:H and a-Si:Ge:F:H and tandem single-gap a-Si:F:H cells.

Figure 9. The effect of 200-keV and 1-MeV proton irradiation on the conversion efficiency of dual-gap, tandem cells of of a-Si:F:H and a-Si:Ge:F:H alloys.

Figure 10. Comparison of the effect of 1-MeV proton irradiation on the efficiency of crystalline Si, GaAs, $CuInSe_2$ and amorphous dual-gap tandem cells.

Figure 11. The effect of 200-keV proton irradiation on the conversion efficiency of tandem, single-gap, a-Si:F:H cells and the effect of subsequent annealing at various temperatures and times.

Figure 12. Ultralight PV system concept for the Space Station. A pair of counter-rotating a-Si alloy arrays deployed by means of centrifugal force.

Figure 13. A design concept for a 1-MW, ultralight PV array.
Volume: 1 cubic meter; area: 100 x 100 meters; thickness: 75 μm;
Voltage: 10,000 Volt; current: 100 A; deployment: 30s.

a. Array in stowed condition
b. Deployment of folded array in x direction
c. Deployment in y direction
d. Fully deployed array

ORIGINAL PAGE IS
OF POOR QUALITY

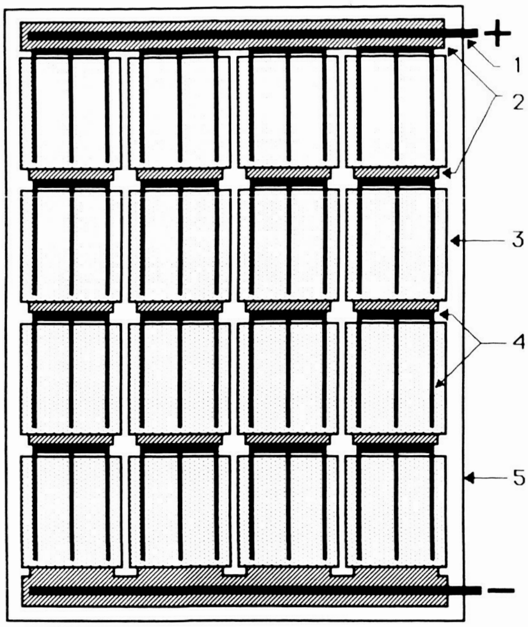

Figure 1. Monolithic module structure consisting of four parallel strings of four series-connected cells in each string.
Legend:
(1) busbar, (2) rear electrode layer, (3) cell, (4) metallic grid, (5) front and rear encapsulant.

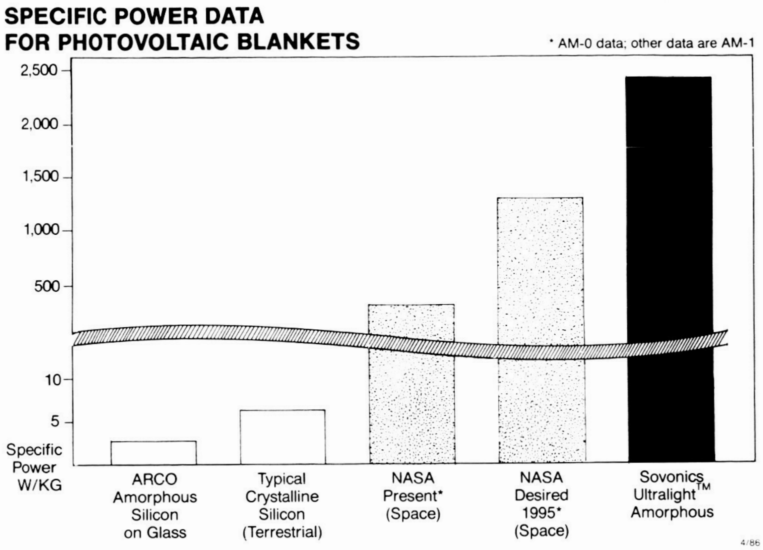

Figure 2

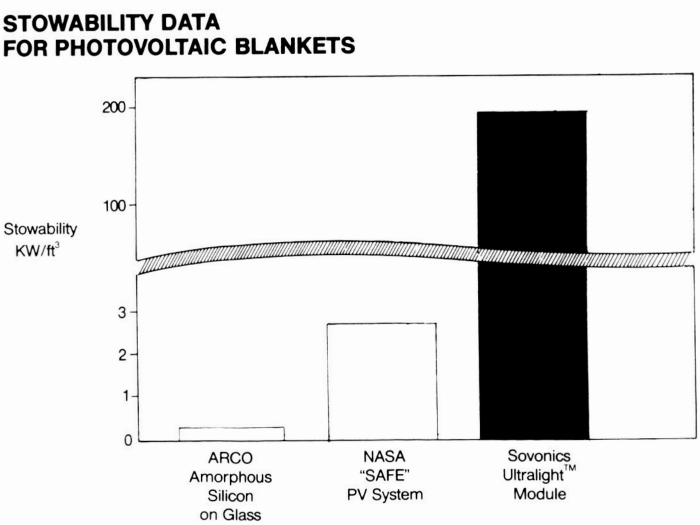

Figure 3

Figure 4

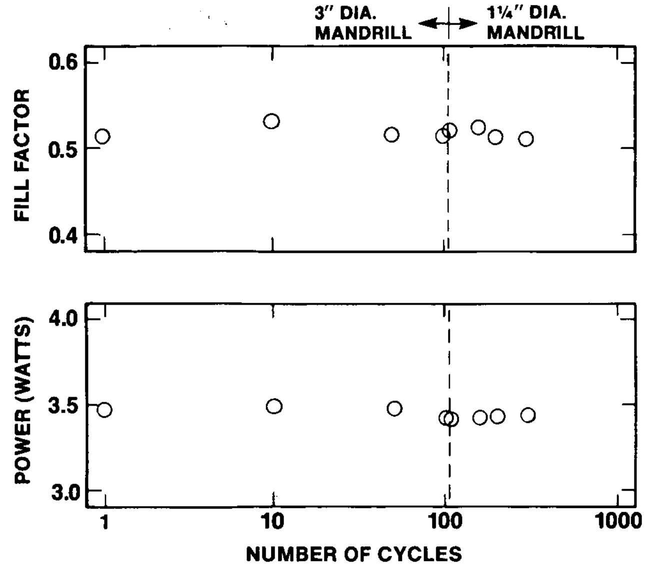

Figure 5

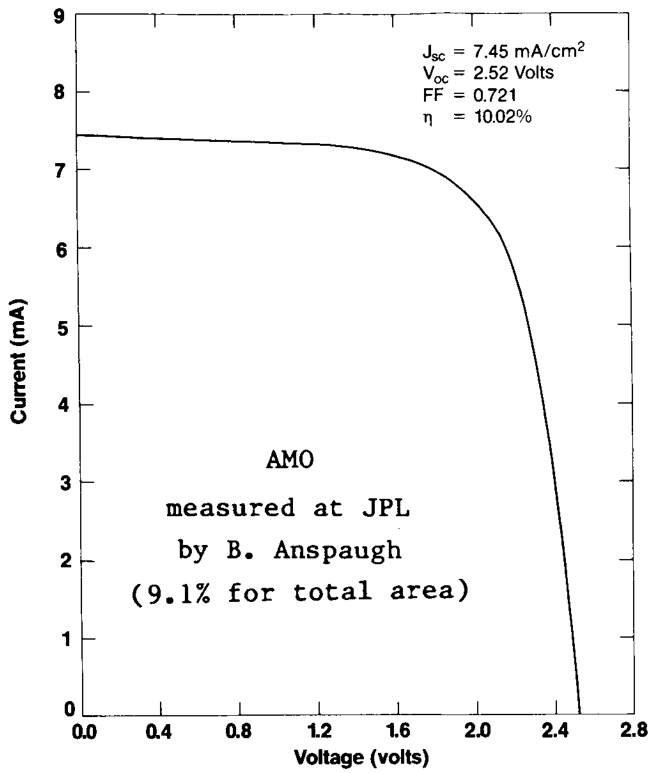

Figure 6

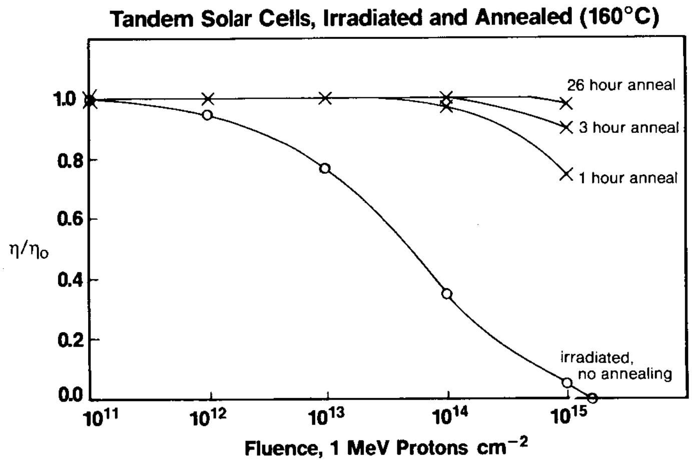

Figure 7

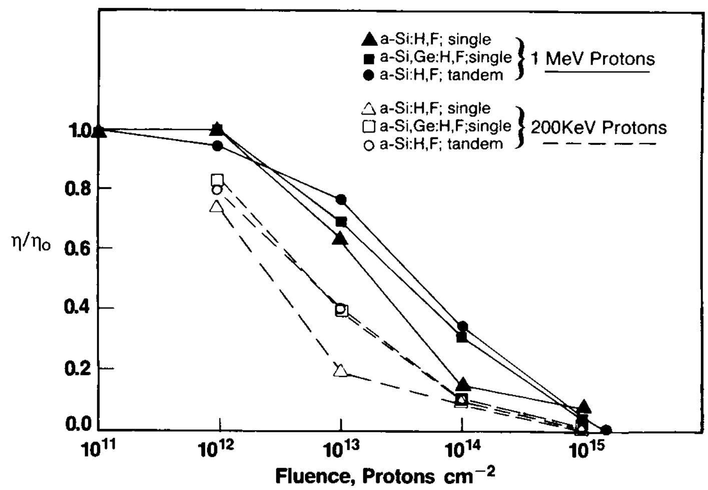

Figure 8

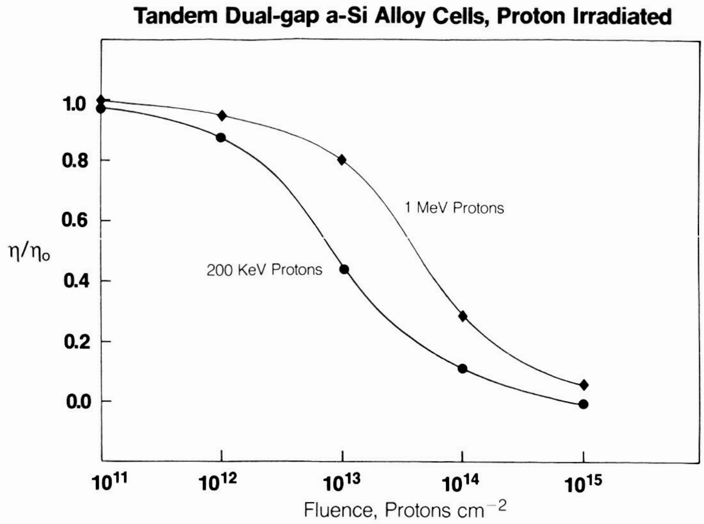

Figure 9

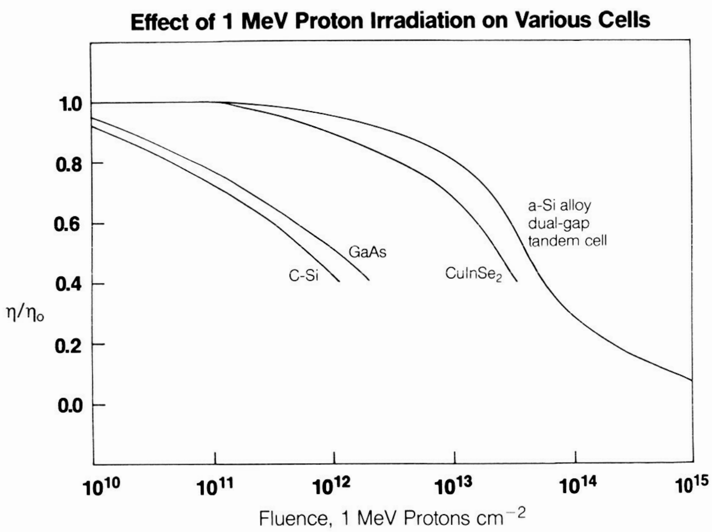

Figure 10

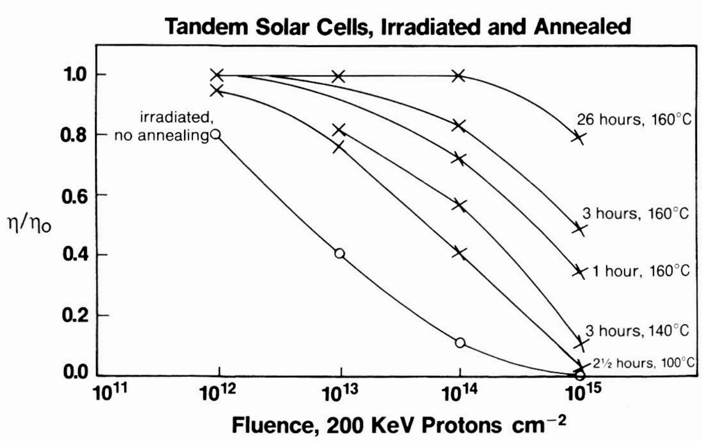

Figure 11

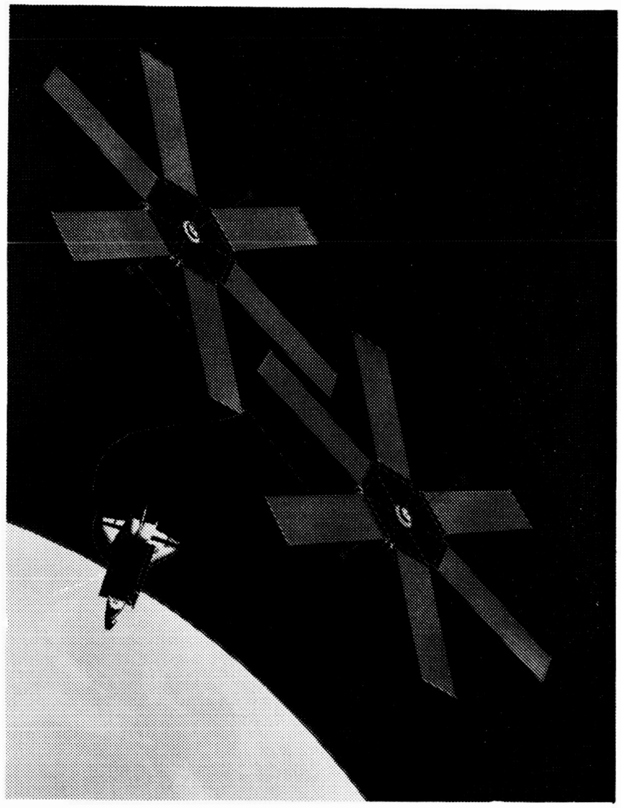

Figure 12

ORIGINAL PAGE IS
OF POOR QUALITY

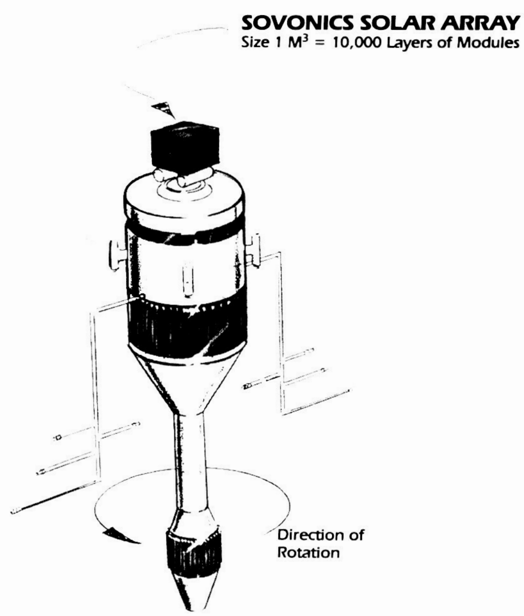

Figure 13 a

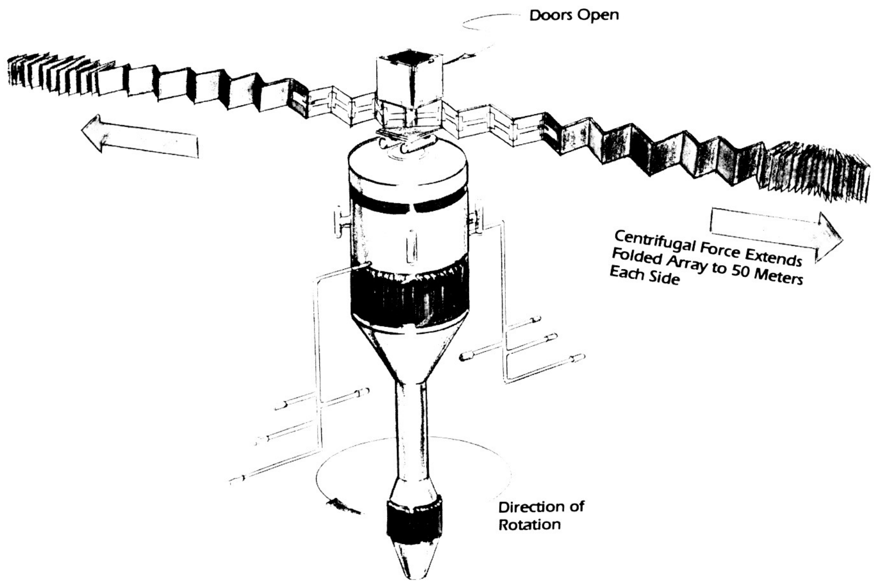

Figure 13 b

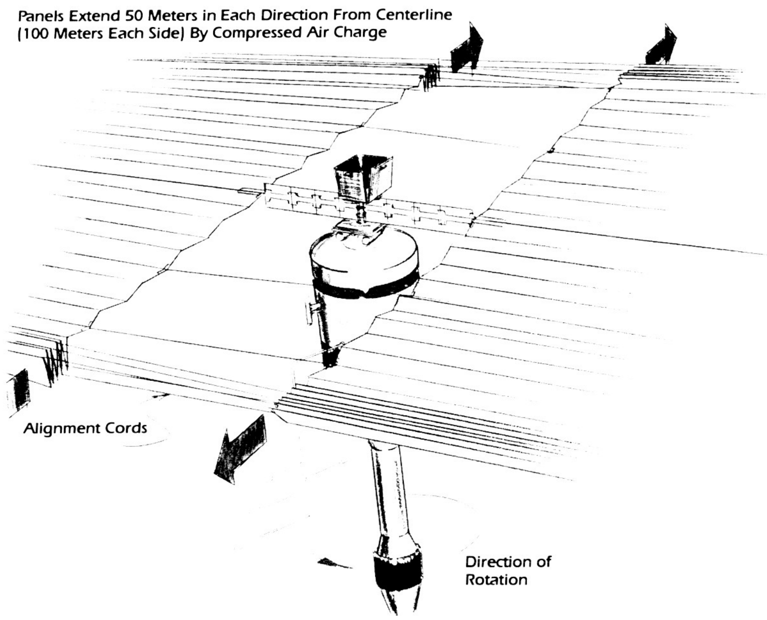

Figure 13 c

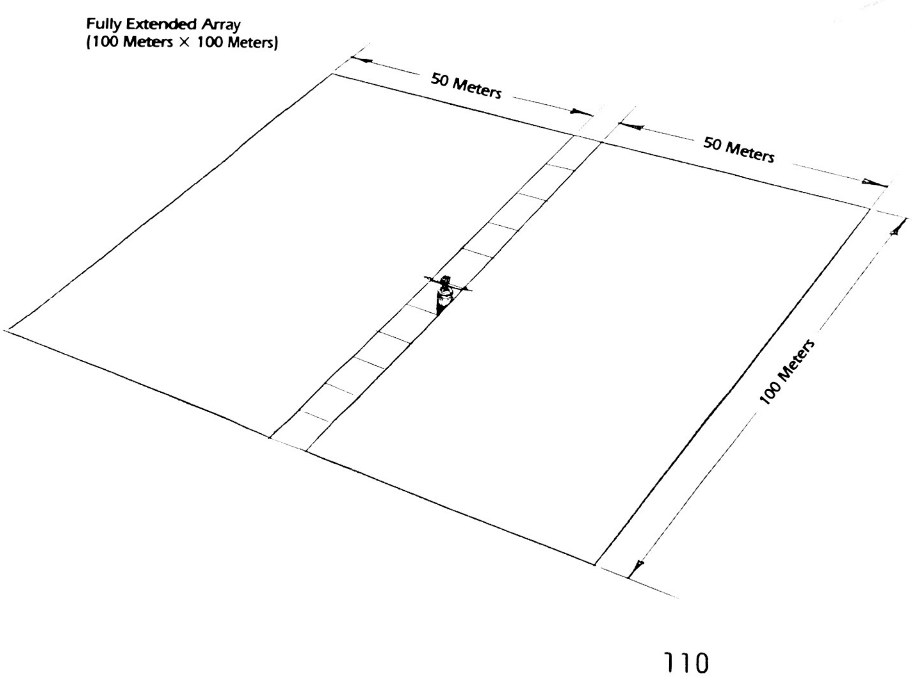

Figure 13 d

ORIGINAL PAGE IS
OF POOR QUALITY